European Journal of Pharmaceutical Sciences 216 (2026) 107383

Contents lists available at ScienceDirect

European Journal of Pharmaceutical Sciences

journal homepage: www.elsevier.com/locate/ejps

Impact of formulation and process parameters on the stability and bioactivity of RNA-loaded lipid nanoparticles during nebulization

Katrin F. Wiebe [a,b], Stefan C. Schneid [c], Werner Hoheisel [d], Wolfgang Frieß [a], Olivia M. Merkel [a,*]

[a] Department of Pharmacy, Pharmaceutical Technology and Biopharmaceutics, LMU Munich, Munich, 81377, Germany
[b] INVITE GmbH, Leverkusen, 51368, Germany
[c] Bayer AG, Pharmaceuticals, CMC Drug Product, Wuppertal, 42117, Germany
[d] Bayer AG, Formulation Technology, Leverkusen, 51368, Germany

ARTICLE INFO

Keywords:
LNPs
RNA
Inhalation
Nebulization
Stability

ABSTRACT

During the pandemic, lipid nanoparticles (LNPs) became widely established as RNA nanocarriers, and hold the promise of future targeting of a broad variety of previously untreatable diseases. LNPs are mostly administered invasively via intramuscular or intravenous injections. Given the lung's large surface, high vascularization and low nuclease abundance, inhalation offers a promising alternative for both local and systemic delivery of LNPs. Vibrating mesh nebulizers present a patient-friendly, high-dose delivery platform. However, the nebulization process imposes thermal and mechanical stress on the LNP formulation. This study contributes to a better understanding of how nebulization affects the physicochemical properties and biological activity of LNPs, depending on formulation and process parameters. We investigated the impact of formulation and process variables such as temperature, concentration, buffer type, and RNA modality on LNP properties including particle size distribution, zeta potential, *in vitro* activity, and RNA integrity. While aggregating, siRNA LNPs protected the encapsulated RNA from degradation, and preserved biological function. In contrast, after the nebulization of mRNA LNPs the cargo was degraded and the biological function diminished. This observation can possibly be attributed both to the higher sensitivity of mRNA toward physical and chemical degradation, and the cargo-dependent morphology of LNPs. While demonstrating that siRNA LNPs preserved their most important characteristics, namely RNA integrity and biological function, our findings emphasize the need for route-specific optimization of LNPs, which need to meet different critical quality criteria when used for inhalation rather than injection.

1. Introduction

Over the last decades, and especially accelerated by the COVID-19 pandemic, RNA has become a focus in the search for new active pharmaceutical ingredients (APIs). Among the various naturally occurring RNA types, two important pharmaceutical modalities are small interfering RNA (siRNA) and messenger RNA (mRNA), used either to silence or to express target genes transiently. (Kandil et al., 2019; Merkel and Kissel, 2011; Xu et al., 2021)

RNA offers potential treatment or prevention of disease targets previously untreatable combined with a comparably short development time. As RNA molecules are hydrophilic, charged, comparably large, prone to hydrolysis, and substrates for ubiquitous nucleases, stability and delivery challenges must be overcome for clinical applications. (Lam et al., 2012; Merkel et al., 2011)

Delivery vectors such as lipid nanoparticles (LNPs) protect RNA cargo from degradation, facilitate cellular uptake, and promote endosomal escape. (Kandil et al., 2019) LNPs are complex formulations, typically consisting of an ionizable lipid that electrostatically interacts with the RNA cargo, complemented with rigidity regulating cholesterol, stabilizing PEGylated lipids, as well as helper lipids. (Hald Albertsen et al., 2022)

Currently, all RNA LNP formulations approved by health authorities are administered either intravenously, as in case of Onpattro®, or intramuscularly, as performed with the SARS-CoV 2 vaccines Comirnaty® and Spikevax®. (Curreri et al., 2023) Systemically administered

* Corresponding author at: LMU Munich, Department of Pharmacy, Butenandtstraße 5 81377 Munich, Germany.
E-mail address: Olivia.merkel@lmu.de (O.M. Merkel).

https://doi.org/10.1016/j.ejps.2025.107383
Received 6 August 2025; Received in revised form 31 October 2025; Accepted 17 November 2025
Available online 19 November 2025

LNPs predominantly accumulate in the liver. (Chen et al., 2016) Specific organ targeting following systemic delivery has been reported with specific lipid components as formulated in SORT LNPs (Dilliard et al., 2021; Wei et al., 2023), although significant research is still required to bring this mechanism to the patient and safety concerns are raised about clogging of lung capillaries. (Omo-Lamai et al., 2024)

Due to its large surface, high vascularization, and low occurrence of nucleases, the lung is an excellent site for local and direct RNA delivery. (Carneiro et al., 2023; Kandil et al., 2019; Lam et al., 2012) Additionally, clinical and preclinical RNA medicines show promise in a broad variety of lung diseases, including infectious diseases such as COVID-19, pneumonia, and tuberculosis, as well as non-transmittable diseases, including bronchial asthma, chronic obstructive lung disease, lung fibrosis, or lung cancer. (Hald Albertsen et al., 2022; Omo-Lamai et al., 2024) Local application of powder or liquids is less invasive, requires a lower dose, and leads to fewer side effects, all of which could also improve patient adherence.

In contrast to other lung administration devices, nebulization does not require breath-hand coordination or deep inspiration, thus making it suitable for patient groups struggling with coordination or compromised inspiration. Additionally, nebulization does not require a propellant, and larger doses can be delivered compared to dry powder inhalers and metered dose inhalers. (Elphick et al., 2015; Neary et al., 2024; Newman, 2005) Among the three main types of nebulizers - jet, ultrasonic and vibrating mesh - the latter is the most commonly used one for RNA nebulization. (Kim et al., 2022; Lokugamage et al., 2021; Neary et al., 2024; van Rijn et al., 2023) In vibrating mesh nebulizers, a piezoelectric crystal vibrates the mesh, resulting in the aerosolization of the aqueous drug formulation. This process, however, increases device and reservoir temperature, generates shear stress and overall energy intake, and can lead to instability, RNA cargo release, particle aggregation and decrease in biological function. (Hertel et al., 2014; Kim et al., 2022; Klein et al., 2021; Lokugamage et al., 2021; van Rijn et al., 2023; Zhang et al., 2020)

This work systematically investigates the effect of vibrating mesh nebulization on the physicochemical characteristics and biological activity of established RNA LNP formulations. It focuses on the influence of formulation and process factors including buffer substances, LNP concentration, temperature, nebulization device and RNA type to contribute to a better understanding of how nebulization impacts LNP integrity and function.

With LNPs containing siRNA and mRNA, two of the currently most relevant RNA types are compared. These two types differ regarding size and stability. To understand the influence of the choice of device, two different commercially available vibrating mesh nebulizers were investigated: the PARI eflow rapid and the Aerogen Pro. While both devices produce aerosols in the desired droplet size range of 1 – 5 μm (Muller et al., 2025), they differ in geometry, residual volume and energy intake. The Aerogen nebulizer is designed to nebulize vertically or slightly angled with the feed solution on top of the vibrating mesh, with almost no residual volume remaining in the reservoir. Due to its geometry, the PARI device retains a larger residual volume – most likely developed to buffer the temperature increase due to energy intake during nebulization (Hertel et al., 2014). Additionally, the mesh is oriented in a 90-degree angle regarding the feed solution. With 35 ± 12 J/g, the overall energy intake has been determined to be larger for the PARI device compared to the Aerogen device with 18 ± 6 J/g (van Rijn et al., 2023).

2. Material and methods

2.1. LNP preparation

Enhanced green fluorescent protein (EGFP) gene was used as a reporter gene for both siRNA and mRNA LNPs. Commercial GFP siRNA (Table 1) was obtained from Merck (Darmstadt, Germany), and mRNA (sequence in the supplement) was obtained from Ribopro (Oss, The Netherlands).

Three different LNP formulations were prepared based on the Onpattro®-, Comirnaty®-, and Spikevax®-formulations. The different lipids were separately dissolved in absolute ethanol (Thermo Fisher Scientific, Waltham, USA), combined in specific lipid molar ratios, and diluted to 2 mM for siRNA LNPs, and 1 mM for mRNA LNPs (Table 2). RNA was diluted in 25 mM sodium acetate (Merck, Darmstadt, Germany) buffer at pH 4.0. For siRNA LNPs, the solutions were mixed using the Impingemet Jet Mixer NanoScaler (Knauer, Berlin, Germany), or a herringbone mixer (microfluidic ChipShop, Jena, Germany) operated with syringe pumps at a total flow rate of 3 ml/min following a ratio of 3:1 (RNA:lipids solution) to achieve a Nitrogen-to-Phosphate (N/P) ratio of 3. mRNA LNP precursors were formulated via a T-Mixer (Techlab, Braunschweig, Germany) operated with syringe pumps following the flow rate parameters stated above, adjusted to N/P 6. Dialysis was performed in Pur-A-Lyzer Maxi 3500 dialysis kits (Merck, Darmstadt, Germany) against PBS (Thermo Fisher Scientific, Waltham, MA, USA) or 0.9 % NaCl (Merck, Darmstadt, Germany) at 4 °C overnight. The resulting LNPs were filtered with a 0.2 μm Supor ® Membrane filter (PALL, New York, NY, USA) and stored at 4 °C.

Table 2
Lipid molar ratios used in the preparation of LNP formulations.

Lipid type	Lipid name	Molar ratio (% mol)
Onpattro®-like (siRNA)		
Ionizable lipid	O-(Z,Z,Z,Z-heptatriaconta-6,9,26,29- tetraem-19-yl)- 4-(N,N-dimethylamino)butanoate (D-Lin-MC3-DMA; MedChemExpress, Monmouth Junction, NJ, USA)	50.0
Helper lipid	1,2-distearoyl-*sn*-glycero-3phosphocholine (DSPC, Avanti Polar Lipids, Alabaster, AL, USA)	10.0
PEG lipid	1,2-dimyristoyl-rac-glycero-3-methoxypolyethylene glycol-2000 (DMG-PEG; Avanti Polar Lipids, Alabaster, AL, USA)	1.5
Sterol	Cholesterol (Merck, Darmstadt, Germany)	38.5
Comirnaty®-like (mRNA)		
Ionizable lipid	((4-Hydroxybutyl)azanediyl)bis(hexane-6,1-diyl)bis (2-hexyldecanoate) (ALC-0315; Avanti Polar Lipids, Alabaster, USA)	46.3
Helper lipid	DSPC	9.4
PEG lipid	6-((2-hexyldecanoyl)oxy)-N-(6-((2-hexyldecanoyl) oxy)hexyl)-N-(4-hydroxybutyl)hexan-1-aminium (ALC-0159; Avanti Polar Lipids, Alabaster, USA)	1.6
Sterol	Cholesterol	42.7
Spikevax®-like (mRNA)		
Ionizable lipid	1-Octylnonyl 8-((2-hydroxyethyl)(6-oxo-6-(undecyloxy)hexyl)amino)octanoate (SM-102; MedChemExpress, Monmouth Junction, USA)	50.0
Helper lipid	DSPC	10.0
PEG lipid	DMG-PEG	1.5
Sterol	Cholesterol	38.5

Table 1
GFP siRNA sequence.

5′	5Phos/rArCrCrCrUrGrArArGrUrUrCrArUrCrUrGrCrArCrCrArCCG	3′
5′	rCrGrGrUrGrGrUrGmCrAmGrAmUrGmArAmCrUmUrCmArGmGrGmUmCmA	3′

2.2. Nebulization

Nebulization of LNPs was performed using two vibrating mesh nebulizers: the PARI eFlow rapid (PARI, Starnberg, Germany) and the Aerogen Pro (Aerogen, Galway, Ireland). For each experiment, 2.5 ml of formulation was nebulized using the PARI device, and 1.0 ml was used with the Aerogen device. The nebulized sample was collected in an ice-cooled tube, which was attached directly to the device. Whenever necessary, samples were stored at 5 °C. Unless otherwise stated, samples were nebulized precooled. If necessary, LNPs were diluted in their respective dispersants before nebulization. All concentrations refer to the calculated amount of RNA.

2.3. Aerosol analysis via laser diffraction

The influence of LNPs on the droplet size of the nebulized aerosol was analyzed via laser diffraction. Particles were prepared as described and diluted in PBS and NaCl, respectively. Pure 0.9 % NaCl and PBS were compared to Spikevax-like and Comirnaty-like mRNA LNPs in PBS (3 ng/µl) as well as siRNA LNPs in PBS (8 ng/µl, and 20 ng/µl), and in 0.9 % NaCl (20 ng/µl). The two nebulizers were attached to the HELOS laser diffractor (Sympatec, Clausthal-Zellerfeld, Germany) equipped with an INHALER module and R2 lens via a customized silicone mouthpiece. For the Aerogen device, an Aerogen T-piece was installed between nebulizer and inhaler module. This held the nebulizer upright and ensured air intake for a suitable optical density. The PARI nebulizer was attached directly without a T-piece. To adjust optical density for PARI measurements, the air control valves on the side of the chamber were set to 6–7 for all measurements. An air flow of 13.9 l/min corresponding to a pressure of 4 mbar was created. Each measurement was carried out in triplicate. Signal integration time was 5 s, and the droplet size was determined as volume-based median diameter following Mie-theory via PAQXOS software (Sympatec, Clausthal-Zellerfeld, Germany).

2.4. Physicochemical analysis

For each nebulization experiment, a corresponding non-nebulized sample was analyzed as reference. Particle size and zeta potential were determined via dynamic light scattering (DLS) and phase analysis light scattering (PALS) using a Zetasizer ultra (Malvern Pananalytical, Malvern, UK). Complementary size data was collected via nanoparticle tracking analysis (NTA) using a NanoSight NS300 (Malvern Panalytical, Malvern, UK). NTA data was sorted by a customized Python program (Python Software Foundation, Beaverton, OR, USA) to exclude all values above the respective size distribution's D90 value. The entire size distribution can be found in the supplement (Figure S1 and S2).

The amount of RNA released from the LNPs during nebulization was quantified via RiboGreen assay and normalized by the results of the corresponding non-nebulized sample. In a black flat bottom 384-well plate, samples were diluted in Tris-EDTA (TE) buffer (Merck, Darmstadt, Germany) at a ratio of 1:1. RiboGreen reagent (Invitrogen Quant-it RiboGreen, Thermo Fisher Scientific, Waltham, MA, USA) was diluted 100-fold in TE buffer and added to the samples at a ratio of 1:1. The plate was shaken for 60 to 90 s and analyzed using the Spark Multimode Microplate Reader (Tecan Group AG, Männedorf, Switzerland). The concentration of non-encapsulated RNA was determined using a calibration curve and normalized to the blank. The relative amount of RNA released from LNPs (R) during nebulization was determined using the following equations:

Equation 1: RNA release

$$R = \frac{EE(non\ nebulized) - EE(nebulized)}{EE(non\ nebulized)}$$

With

$$EE = \frac{c(RNA, calculated) - c(RNA,\ non\ encapsulated)}{c(RNA,\ calculated)}$$

Where

EE: encapsulation efficiency [%]
c: concentration [ng/µl]
R: RNA release [%]

2.5. Biological activity

The biological activity of nebulized LNPs was determined by measuring siRNA-mediated gene silencing and mRNA-induced protein expression. Gene expression experiments were conducted in H1299 cells cultivated in RPMI media (Sigma Aldrich, Taufkirchen, Germany) supplemented with 10 % fetal bovine serum (FBS; Thermo Fisher Scientific, Darmstadt, Germany), and 1 % Penicillin-Strepotmycin (Thermo Fisher Scientific, Darmstadt, Germany). For gene silencing, eGFP expressing H1299 cells were cultivated as stated above with the addition of 0.4 % G418 (Merck, Darmstadt, Germany).

For gene silencing experiments, 25,000 EGFP expressing H1299 cells were seeded 24 h before transfection and treated with nebulized LNPs at a calculated dose of 50 pmol RNA per well. Non-nebulized LNPs were used as the control and untreated cells were used as the blank. After an incubation of 48 h, the cells were washed with PBS (Merck, Darmstadt, Germany), harvested with 0.05 % Trypsin (Thermo Fisher Scientific, Waltham, MA, USA), and washed again before measuring with an Attune Nxt Flow Cytometer (Thermo Fisher Scientific, Waltham, MA, USA) operated with Attune Cytometric Software (Thermo Fisher Scientific, Waltham, MA, USA). Median fluorescence intensity (MFI) of eGFP protein expression was measured using a 488 nm excitation laser and a 530/30 emission filter. Gates were set to ensure a minimum of 10,000 viable cells per sample.

For the protein expression experiments, 25,000 H1299 wildtype cells were seeded 24 h before transfection with nebulized and non-nebulized LNPs at a calculated dose of 300 ng RNA per well. After an incubation of 24 h, flow cytometry analysis was performed as described above.

2.6. Bioanalyzer microfluidic gel electrophoresis

Microfluidic automated gel electrophoresis was conducted using a Bioanalyzer (Agilent, Santa Clara, *CA*, USA). For every experiment, free RNA was treated exactly as the LNP samples and analyzed as a control. Prior to electrophoresis, RNA was precipitated with ice-cooled 60 mM ammonium acetate (Merck, Darmstadt, Germany) in HPLC grade isopropanol (Merck, Darmstadt, Germany). Samples were then gently vortexed and centrifuged at 20,000 g for 20 min at 4 °C. The supernatant was removed, and the pellet was washed with ice-cooled isopropanol, followed by vortexing and centrifugation using the same settings. After removing the supernatant, the pellets were dried at room temperature under vacuum (20 mbar) in a vacuum oven (Memmert, Schwabach, Germany) for 30 min, and resuspended in RNase-free water (Carl RothGmbH + Co. KG, Karlsruhe, Germany). RNA was heat-denaturized in a 70 °C heating block for 2 min (without shaking) and immediately placed on ice. mRNA samples were analyzed on the same day, whereas siRNA samples were stored at −20 °C overnight before analysis.

The Agilent 'Small RNA Kit' was used for siRNA samples, and the 'Pico 6000 RNA' Kit was used for mRNA. The Agilent Expert 2000 software was used for conducting electrophoresis and data analysis.

2.7. Statistical analysis and graphs

Statistical analysis and creation of graphs were performed with PRISM 5 (GraphPad Software, Boston, USA). If not stated otherwise, each data point represents the mean of triplicates, and the error bars

present the corresponding standard deviation. Statistical significance was determined via one-way ANOVA with subsequent Bonferroni test (not significant (ns): $P \geq 0.05$,

*: $P \leq 0.05$, **: $P \leq 0.01$, ***: $P \leq 0.001$). If not stated otherwise, all significance indicators refer to the comparison with the respective non-nebulized sample.

3. Results and discussion

To better understand the impact of vibrating mesh nebulization, Onpattro-like LNPs carrying siGFP-RNA were nebulized using both the PARI eFlow Rapid and Aerogen Pro nebulizers in 0.9 % NaCl and PBS (pH 7.4). The siRNA concentration was 20 ng/µl in both NaCl and PBS, and an additional concentration of 8 ng/µl was tested in PBS. To investigate the influence of temperature, one data set (PBS, 8 ng/µl, room temperature (RT)) was obtained using LNPs warmed to room temperature immediately before nebulization. mRNA LNPs (Spikevax-like and Comirnaty-like) were nebulized in PBS pH 7.4 at a concentration of 3 ng/µl.

3.1. Aerosol analysis by laser diffraction

A droplet size between 1 and 5 µm is widely recognized as suitable for pulmonary deposition (Szabova et al., 2021), and both nebulizer devices used in this work are known to generate aerosols of 0.9 % NaCl within this size range (Kim et al., 2023; Heiser et al., 2025). To assess whether the LNP formulations affect droplet size, laser diffraction analysis was performed (Table 3). The droplet sizes measured for 0.9 % NaCl were consistent with literature values, and similar droplet sizes were observed for PBS. The addition of LNPs did not have a relevant effect on droplet size, indicating that our formulations would deposit in the lung to a high fraction upon inhalation.

3.2. Physicochemical properties

DLS data showed a significant size increase for all samples, regardless of device, dispersant, concentration or temperature (Fig. 1A), which is confirmed by NTA data (Fig. 1B). The size distribution did not shift uniformly but broadend, as demonstrated by an increase in PDI in DLS and the widening of the size distribution in NTA. Zeta potentials showed no significant change for all samples (Table 4). In contrast to certain liposome formulations that can dissassemble during and reassemble after nebulization (Szabova et al., 2021), the size increase observed here occuring without a change in zeta potential indicated LNP aggregation rather than larger particle formation. RNA release (Equation 1) from the LNPs during nebulization was determined via the Ribogreen assay. While it was not possible to obtain reliable data in NaCl, some RNA release was detected in PBS samples at both low and high RNA concentrations (Table 4).

Table 3
Droplet size as volume-based median diameter (VMN [µm]). Samples were prepared in 0.9 % NaCl or PBS and analyzed with each nebulizer. No significant differences were observed between dispersants or between devices; significant differences between a nebulized sample and its corresponding dispersant and nebulizer are indicated by * ($p < 0.05$).

Sample	Aerogen Pro	PARI eFlow rapid
0.9 % NaCl	4.77 ± 0.06	4.85 ± 0 03
PBS	4.79 ± 0.02	4.80 ± 0.06
siRNA LNPs in NaCl, 20 ng/µl	4.84 ± 0.02	4.66 ± 0.07
siRNA LNPs in PBS, 20 ng/µl	4.83 ± 0.04	4.52 ± 0.12
siRNA LNPs in PBS, 8 ng/µl	4.77 ± 0.09	4.43 ± 0.07 (*)
Comirnaty-like mRNA LNPs in PBS, 3 ng/µl	4.83 ± 0.05	4.90 ± 0.03
Spikevax-like LNPs in PBS, 3 ng/µl	4.71 ± 0.21	4.40 ± 0.30 (*)

3.3. Influence of buffer components

At first glance, the size increase trends for NaCl and PBS samples seemed similar. However, a closer examination of the NTA results revealed differences: in PBS samples, the overall shape of the size distribution remained largely unchanged, with relatively few particles widening the distribution and thereby causing a minor increase in the median size value. In contrast, the size distribution of the NaCl samples broadened more distinctly with a higher proportion of large particles that considerably shifted the median size to larger values. While the ionic strength of both solutions is similar, the additional buffering agents in PBS appeared to limit the amount of aggregation induced by nebulization.

3.4. Influence of LNP concentration

While the trends remained consistent across all PBS samples, significantly less RNA was released in the 8 ng/µl samples compared to the 20 ng/µl samples not only in absolute but also in relative terms (Table 4). Additionally, the size increase was less pronounced at lower concentrations, where the probability of particle-particle interactions leading to aggregation is decreased. If therapeutic efficacy can be maintained at lower concentration within a suitable delivery volume, this approach could be advantageous and should be considered.

3.5. Influence of sample temperature

One possible explanation for the observed changes in LNP properties is the considerable heat generated by vibrating mesh nebulizers (Hertel et al., 2014). To minimize this effect, all samples were nebulized after being precooled (5 °C). Yet, comparison of precooled with RT formulations showed no impact of temperature on size increase or RNA release. These findings suggest that precooling does not significantly change the nebulization process and is insufficient to prevent aggregation.

Factors such as shear, surface interactions within the device, or air-liquid interfacial stress, may play a more dominant role in destabilizing the LNPs during nebulization. In a recent publication, Kim et al. demonstrated that for siRNA-encapsulating LNPs containing >0.5 % PEG lipid, neither heat nor mechanical stress alone lead to permanent aggregation (Kim et al., 2023). Together with our findings (the formulation contained 1.5 % PEG) this indicates that a combination of stress factors is responsible for LNP aggregation during nebulization.

Future investigations could explore how device design, droplet generation rate, and material compatibility contribute to these effects and LNP aggregation. Understanding and mitigating these destabilization mechanisms is crucial for preserving LNP integrity and ensuring consistent therapeutic outcomes in inhaled siRNA delivery. Additionally, modifying LNP composition or incorporating stabilizing excipients like Poloxamer 188 (Heiser et al., 2025) might offer more robust protection against structural changes during aerosolization.

3.6. Biological activity

The biological activity of LNPs containing 8 ng/µl siRNA in PBS was tested as a representative formulation in EGFP-expressing H1299 cells. A marked gene knockdown was observed for both non-nebulized and nebulized LNPs (Fig. 1C). Since no significant difference in fluorescence intensity was detected between the two groups, it can be concluded that the siRNA remains protected within the LNPs and the amount of siRNA released from the particle during nebulization is negligible. These results indicate that, despite the physicochemical changes observed post-nebulization such as size increase, the functional integrity of the siRNA payload was maintained. Together with the unchanged zeta potential, this suggests that the LNPs retained their structural ability to deliver siRNA effectively via the facilitation of cargo protection, cellular

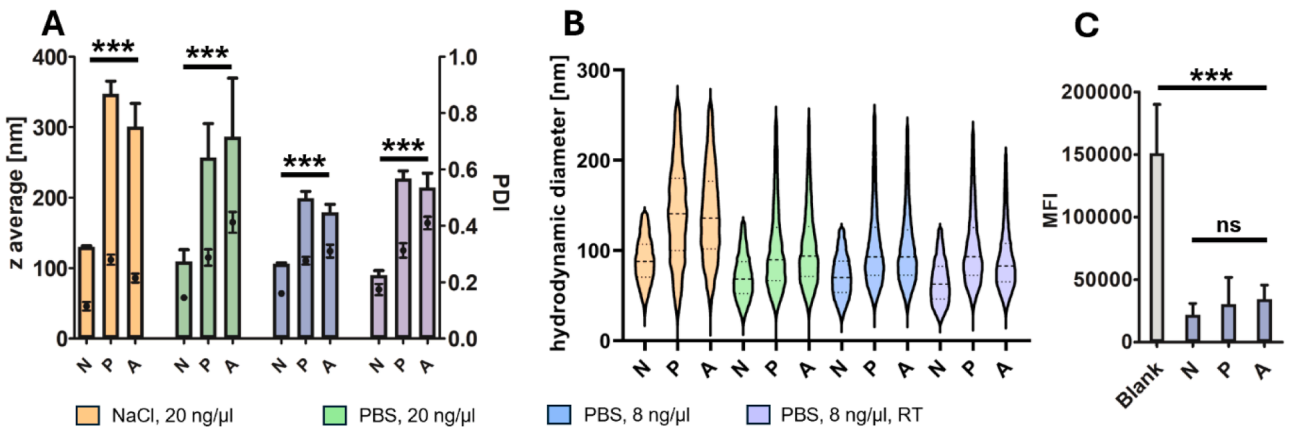

Fig. 1. Physicochemical characteristics of non-nebulized and nebulized siRNA LNPs. N: non-nebulized, P: nebulized via PARI eflow rapid, A: nebulized via Aerogen Pro. (A) DLS particle size data: z average is shown as bars, and polydispersity index (PDI) as dots. Indicated statistical significance refers to the comparison with the corresponding non-nebulized sample (N). The comparison between the two nebulizers was not significant for any of the samples. B: NTA particle size data. Dashed lines represent the median, dotted lines the quartiles. To improve clarity, the violin plot displays the distribution of all particles below the respective D90 value. The entire size distribution can be found in the supplement (Figures S1 and S2). C: *In vitro* gene knockdown of EGFP in H1299 cells using LNPs loaded with 8 ng/µl siRNA in PBS. MFI: Median Fluorescence Intensity. Indicated statistical significance refers to the comparison with the blank, and the non-nebulized sample (N), respectively.

Table 4
RNA release and zeta potential values for siRNA LNPs. Zeta potential data differences were not statistically significant. Statistical significance for RNA release data is indicated below.

Sample	RNA releasemean ± SD [%]		Zeta potential mean ± SD [mV]		
	P	A	N	P	A
siRNA LNP, **20** ng/µl, 0.9 % **NaCl**	No reliable data obtained		10.3 ± 2.0	8.4 ± 1.7	10.9 ± 1.4
siRNA LNP, **20** ng/µl, **PBS** pH 7.4	15.9 ± 2.8 [a,b]	13.8 ± 3.4 [a,f]	12.0 ± 5.0	10.2 ± 5.1	10.1 ± 4.5
siRNA LNP, **8** ng/µl, **PBS** pH 7.4	6.4 ± 1.9 [b,c,d]	6.4 ± 2.4 [c,f,g]	6.7 ± 3.4	7.1 ± 1.5	8.9 ± 1.3
siRNA LNP, **8** ng/µl, **PBS** pH 7.4, **RT**	7.4 ± 4.6 [d,e]	1.0 ± 0.7 [e,g]	9.2 ± 5.3	9.7 ± 3.5	8.5 ± 2.1

a: ns, b: ***; c: ns, d: ns, e: *, f: **, g: ns.

uptake and endosomal escape, even after exposure to the mechanical stress of vibrating mesh nebulization. Importantly, this supports the feasibility of using such devices for pulmonary delivery of siRNA therapeutics, where maintaining biological activity after aerosolization is critical.

3.7. Impact of nebulization on different RNA types

To understand the impact of nebulization on different RNA types, mRNA encapsulating LNPs with Comirnaty-like and Spikevax-like formulation were nebulized at 3 ng/µl in PBS. Similar to siRNA LNPs, a significant particle growth was detected for both formulations (Fig. 2A). NTA data (Fig. 2B) confirmed a broadening of size distribution aligning with particle aggregation. Generally, mRNA LNPs showed more pronounced aggregation compared to siRNA LNPs upon nebulization.

As observed with siRNA LNPs, the zeta potential did not change significantly in either formulation (Table 5), indicating no major rearrangement at the particles' surface. Li et al. describe a particle size increase accompanied by a zeta potential shift (Li et al., 2025). Given their preparation method and initial zeta potential values, the authors expect the mRNA to be present on the outside of the particles, which allows for a rearrangement during nebulization. With our microfluidics approach the mRNA is far and foremost located inside the LNPs and the structure remains unchanged upon nebulization.

The amount of RNA released from mRNA LNPs appears to be lower than that from siRNA LNPs (Table 5). Interestingly, nebulization with the PARI nebulizer resulted in a lower amount of RNA being released after nebulization compared to the Aerogen device, for both Comirnaty- and Spikevax-like LNPs, suggesting that the PARI nebulizer may be gentler on these LNPs. However, this trend is not consistent with the *in vitro* expression data. Although expression efficiency in H1299 was strongly reduced following nebulization, it remained detectable across all formulation and devices (Fig. 2C and D). Especially for Spikevax-like LNPs, no difference was observed between expression after PARI or Aerogen nebulization.

While the physicochemical properties of siRNA and mRNA LNPs were comparable, mRNA LNPs appear to be more susceptible to damage due to nebulization. This may be attributed partly to the different properties of the two RNA types. siRNA is relatively short (approximately 20 base pairs) and double-stranded, whereas mRNA is much longer (usually ranging from 2000 – 20,000 base pairs) and single-stranded (Curreri et al., 2023). This leads to mRNA being particularly susceptible to shear stress, such as that generated by vibrating mesh nebulizers. (van Rijn et al., 2023) Additionally, LNP morphology depends on the type of encapsulated RNA. While for siRNA LNPs a more uniform core-shell structure appears to be most likely (Viger-Gravel et al., 2018), mRNA LNPs display so-called bleb-structures (Brader et al., 2021; Schoenmaker et al., 2021) and it has been demonstrated by Brader et al. that additionally to aggregation, these bleb-structures can rupture when mRNA LNPs undergo physical stress (Brader et al., 2021). In a recent publication, Jiang et al. also reported the introduction of randomly stacked lamellar structures after nebulization, indicating a rearrangement of the LNP that could lead to RNA release (Jiang et al., 2024). Moreover, the loss of mRNA containing pockets after nebulization was reported as demonstrated by CryoEM (Heiser et al., 2025).

3.8. RNA integrity

To gain a deeper understanding of how nebulization affects distinct RNA types, RNA integrity was analyzed via Bioanalyzer microfluidic automated gel electrophoresis. The band position of siRNA from nebulized and non-nebulized samples remained unchanged compared to control siRNA (Fig. 3), demonstrating that siRNA was not damaged during the whole preparation and nebulization process. This is also reflected in the electropherograms (Figure S3).

In contrast, both Comirnaty-like and Spikevax-like LNPs exhibited a substantial increase of small mRNA fragments as well as aggregates compared to non-nebulized samples and control mRNA (Fig. 3). This

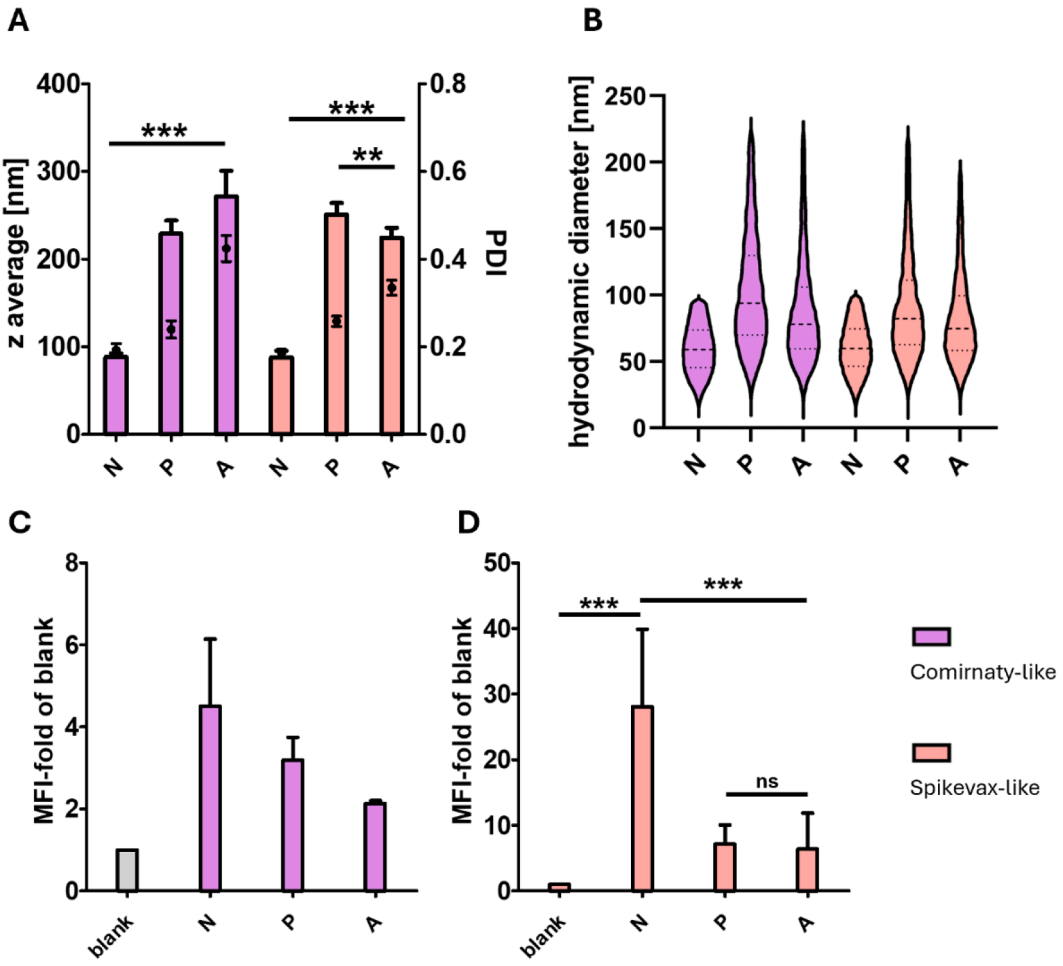

Fig. 2. Characteristics of non-nebulized and nebulized mRNA LNPs. N: non-nebulized, P: nebulized via PARI eflow rapid, A: nebulized via Aerogen Pro. (A) DLS size data: z average is shown as bars, PDI as dots. Indicated statistical significance refers to the comparison with the non-nebulized sample (N). For Comirnaty-like mRNA LNPs, the results of the different nebulizer devices did not differ significantly, for the Spikevax-like LNPs, significance is indicated. B: NTA size data. To improve clarity, the violin plot displays the distribution of all particles below the respective D90 value. The entire size distribution can be found in Figure S1. C: *In vitro* GFP expression in H1299 cells after transfection with Comirnaty-like mRNA LNP in PBS. D: *In vitro* GFP expression in H1299 cells after transfection with Spikevax-like mRNA LNP in PBS. Horizontal significance lines spanning the control and both nebulized samples indicate statistical significance referring to the comparison of both nebulized samples with the non-nebulized sample (N).

Table 5
RNA release and zeta potential values for mRNA LNPs. Neither the differences of RNA release nor that of zeta potential values are statistically significant.

Sample	RNA releasemean ± SD [%]		Zeta potential mean ± SD [mV]		
	P	A	N	P	A
Comirnaty-like mRNA LNPs, **3** ng/µl in **PBS** pH 7.4	0.3 ± <0.1	6.9 ± 0.1	9.9 ± 1.3	8.5 ± 3.0	9.7 ± 0.8
Spikevax-like mRNA LNPs, **3** ng/µl in **PBS** pH 7.4	1.0 ± 0.1	4.8 ± 0.1	8.7 ± 2.1	10.5 ± 1.1	9.6 ± 0.4

underlines the assumption of mRNA being more susceptible to stress-derived degradation.

3.9. Influence of nebulization device

In summary, across all parameters analyzed in this study, the tested nebulization devices did not show a difference in their impact on the physicochemical properties and *in vitro* activity of both siRNA and mRNA LNPs. This is particularly interesting considering the higher energy intake of the PARI nebulizer (van Rijn et al., 2023). It is possible that a threshold in energy intake exists, above which the LNPs are destabilized enough to release their cargo, which will subsequently be degraded. For siRNA LNPs, both nebulizers seem to stay below this threshold, while it is exceeded for mRNA LNPs with both devices. This work underlines that while RNA type, lipid composition, and buffer each play crucial roles in the development of a nebulizable LNP formulation, the choice of devices is less important and, at least for the instruments tested, it is likely that they can be used interchangeably.

3.10. Improving in vitro–in vivo translation for nebulized LNPs

In vitro models often poorly reflect *in vivo* conditions, particularly when relying solely on immortalized cell lines. Consequently, strong *in vitro* performance does not necessarily translate into *in vivo* efficacy (Lindsay et al., 2025). Moreover, a considerable translational gap persists between preclinical and clinical studies, especially for inhaled therapies, where deposition depends on the interplay between aerosol size distribution and airway anatomy (Hickey et al., 2024). To better contextualize our findings within this translational challenge, the influence of LNP on the size of the formed droplets, and thus their potential to reach the human lung, as well as RNA integrity were assessed. Our siRNA LNP formulations were capable of reaching the lungs, maintained RNA integrity, and showed *in vitro* activity. However, since the size influences LNP performance *in vivo* by altering important

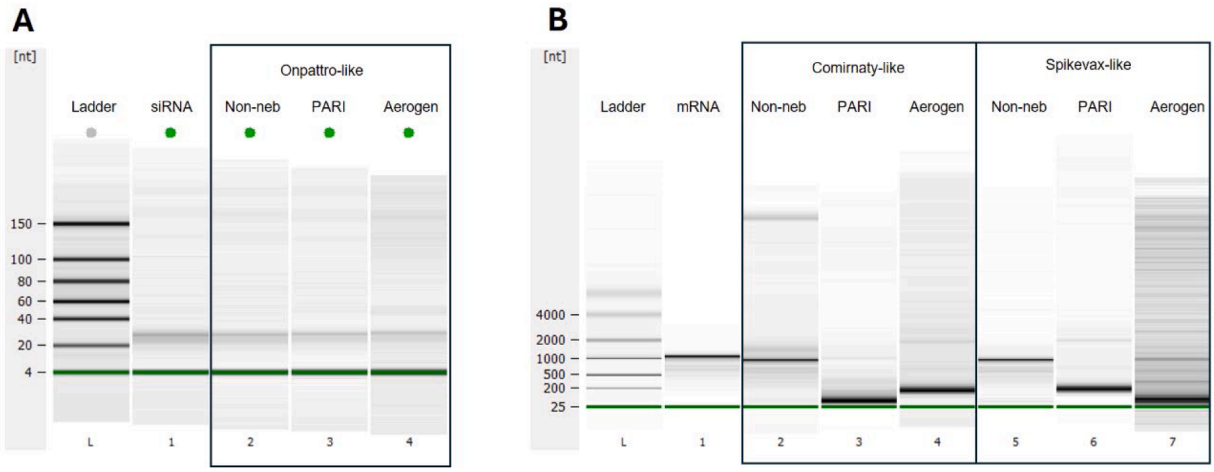

Fig. 3. Gel-like visualization of Bioanalyzer Microfluidic Gel Electrophoresis of non-nebulized and nebulized LNPs ($n = 1$). siRNA/mRNA: RNA control, A: Onpattro-like siRNA LNPs, B: Comirnaty-like mRNA LNPs and Spikevax-like LNPs, N = non-nebulized, P: PARI-nebulized, A: Aerogen-nebulized. Electropherograms of each sample can be found in Figure S2.

aspects such as immunological activation (Hald Albertsen et al., 2022), the demonstrated size increase indicates the need for optimization. In a recent publication, Kim et al. proposed the use of higher PEG-concentrations (3.5 % of the lipid formulation) and beta-sitosterol as an alternative to cholesterol, claiming that the optimized PEG-amount reduces the impact of shear stress and enhances mucus penetration while the alternative sterol improves endosomal escape by providing a polyhedral shape. (Kim et al., 2022) The addition of stabilizing excipients, like Poloxamer 188 (Heiser et al., 2025), and alternative nebulization techniques designed to lower the shear stress (Klein et al., 2021) are additional fields worth investigating.

In the context of *in vitro-in vivo* correlation not only false positives but also false negatives can occur, meaning that formulations performing poorly *in vitro* can still exhibit good efficacy *in vivo* (Xue et al., 2024). This is why poor performance in cell culture studies should not preclude further investigation, instead the underlying reasons for the inadequate *in vitro* performance need to be elucidated. In this case, the mRNA degradation was the reason, indicating the need for further optimization.

When developing alternative administration routes or targeting new organs, conventional cell culture models can be insufficiently predictive. To enhance *in vitro–in vivo* correlation in the inhalative field, we recommend a stepwise approach: from basic cell culture studies using relevant cell lines to more advanced models such as mucus penetration assays, air-liquid interface culture, or precision-cut lung slices (Hickey et al., 2024). To avoid false-negative outcomes, biological assessments should be complemented by a detailed physicochemical characterization of the RNA cargo.

4. Conclusion

In summary, vibrating mesh nebulization alters the physicochemical characteristics of LNPs regardless of the RNA type, lipid composition, dispersant, or concentration tested in this study. This aligns with recently published results on the nebulization of various LNP formulations and liposomes, demonstrating that RNA release and particle size increase during vibrating mesh nebulization are common challenges for many similar formulations. (Klein et al., 2021; van Rijn et al., 2023)

For siRNA-LNPs, physical changes are limited to a size increase which is likely due to aggregation, while RNA integrity and *in vitro* performance remain essentially unchanged. Most importantly, the preserved *in vitro* biological activity demonstrates that siRNA protection, cellular uptake, and endosomal escape properties of the LNPs remain functional after nebulization.

In contrast, mRNA LNPs with their fragmented cargo only mediate greatly diminished gene expression after nebulization. This emphasizes the need for formulation and process optimization, especially to stabilize the more fragile mRNA. Possible improvements require innovative changes to the lipid formulation, the addition of stabilizing agents, or the use of advanced nebulization devices. Further investigation of buffer components, shear stress reduction, and temperature control is recommended to steer the development of formulation and optimized nebulization processes.

Finally, if LNP formulations originally developed for parenteral application are to be adapted for inhalation via nebulization, this work underlines the importance of evaluating deviations in physicochemical properties, RNA integrity and overall LNP performance to optimize formulation and processing accordingly.

LLM statement

During the preparation of this work the authors used ChatGPT in order to improve readability and language. After using this tool, the authors reviewed and edited the content as needed and take full responsibility for the content of the publication.

CRediT authorship contribution statement

Katrin F. Wiebe: Writing – original draft, Visualization, Methodology, Investigation, Formal analysis, Data curation. **Stefan C. Schneid:** Writing – review & editing. **Werner Hoheisel:** Funding acquisition. **Wolfgang Frieß:** Writing – review & editing, Supervision, Resources, Project administration, Funding acquisition. **Olivia M. Merkel:** Writing – review & editing, Supervision, Resources, Project administration, Methodology, Funding acquisition, Conceptualization.

Declaration of competing interest

O.M. is a consultant for Corden Pharma GmbH, AMW GmbH, and for PARI Pharma GmbH. O.M. is advisory board member for Coriolis Pharma GmbH and consultant for AbbVie Deutschland GmbH on unrelated projects. O.M. has equity interests in RNhale GmbH. S.S. and W.H. are employees of Bayer AG and may own stock. K.W. is an employee of INVITE GmbH.

Acknowledgements

The authors would like to thank the Drug Delivery and Innovation

Center (DDIC), INVITE GmbH, Leverkusen, for their financial support and express their gratitude for the fruitful discussions with members of the DDIC.

Special thanks are owed to Simone Carneiro, Sabine Inghelbrecht, Tim Lillotte, Nora Martini, Nelly Mettenbrink, Stefan Schiller, and Benjamin Winkeljann.

Funding: This work was financed by the Drug Delivery Innovation Center (DDIC), INVITE GmbH, Leverkusen (Germany).

Supplementary materials

Supplementary material associated with this article can be found, in the online version, at doi:10.1016/j.ejps.2025.107383.

Data availability

Data will be made available on request.

References

Brader, M.L., et al., 2021. Encapsulation state of messenger RNA inside lipid nanoparticles. Biophys. J. 120 (14), 2766–2770.
Carneiro, S.P., et al., 2023. Shaping the future from the small scale: dry powder inhalation of CRISPR-Cas9 lipid nanoparticles for the treatment of lung diseases. Expert. Opin. Drug Deliv. 1–17.
Chen, S., et al., 2016. Influence of particle size on the in vivo potency of lipid nanoparticle formulations of siRNA. J. Control Rel. 235, 236–244.
Curreri, A., et al., 2023. RNA therapeutics in the clinic. Bioeng. Transl. Med. 8 (1), e10374.
Dilliard, S.A., Cheng, Q., Siegwart, D.J., 2021. On the mechanism of tissue-specific mRNA delivery by selective organ targeting nanoparticles. Proc. Natl. Acad. Sci. U S A 118 (52).
Elphick, M., et al., 2015. Factors to consider when selecting a nebulizer for a new inhaled drug product development program. Expert. Opin. Drug Deliv. 12 (8), 1375–1387.
Hald Albertsen, C., et al., 2022. The role of lipid components in lipid nanoparticles for vaccines and gene therapy. Adv. Drug Deliv. Rev. 188, 114416.
Heiser, B.J., et al., 2025. Systematic screening of excipients to stabilize aerosolized lipid nanoparticles for enhanced mRNA delivery. RSC Pharm.
Hertel, S., et al., 2014. That's cool!–nebulization of thermolabile proteins with a cooled vibrating mesh nebulizer. Eur. J. Pharm. Biopharm. 87 (2), 357–365.
Hickey, A.J., et al., 2024. Practical considerations in dose extrapolation from animals to humans. J. Aerosol. Med. Pulm. Drug Deliv. 37 (2), 77–89.
Jiang, A.Y., et al., 2024. Combinatorial development of nebulized mRNA delivery formulations for the lungs. Nat. Nanotechnol. 19 (3), 364–375.
Kandil, R., et al., 2019. Coming in and finding out: blending receptor-targeted delivery and efficient endosomal escape in a novel bio-responsive siRNA delivery system for gene knockdown in pulmonary T cells. Adv. Ther. (Weinh) 2 (7).
Kim, J., et al., 2022. Engineering lipid nanoparticles for enhanced intracellular delivery of mRNA through inhalation. ACS. Nano 16 (9), 14792–14806.
Kim, K.H., et al., 2023. Biophysical characterization of siRNA-loaded lipid nanoparticles with different PEG content in an aqueous system. Eur. J. Pharm. Biopharm. 190, 150–160.
Klein, D.M., et al., 2021. Degradation of lipid based drug delivery formulations during nebulization. Chem. Phys. 547.
Lam, J.K., Liang, W., Chan, H.K., 2012. Pulmonary delivery of therapeutic siRNA. Adv. Drug Deliv. Rev. 64 (1), 1–15.
Li, H.Y., et al., 2025. Pulmonary delivery of LNP-mRNAs aerosolised by vibrating mesh nebulizer: an emphasis on variations and in-depth analyses of physicochemical properties. Int. J. Pharm. 680, 125796.
Lindsay, S., et al., 2025. Exploring the challenges of lipid nanoparticle development: the In vitro-In vivo correlation gap. Vaccines. (Basel) 13 (4).
Lokugamage, M.P., et al., 2021. Optimization of lipid nanoparticles for the delivery of nebulized therapeutic mRNA to the lungs. Nat. Biomed. Eng. 5 (9), 1059–1068.
Merkel, O.M., et al., 2011. Polymer-related off-target effects in non-viral siRNA delivery. Biomaterials 32 (9), 2388–2398.
Merkel, O.M., Kissel, T., 2011. Nonviral pulmonary delivery of siRNA. Acc. Chem. Res. 45, 961–970.
Muller, J.T., et al., 2025. Nebulization of RNA-loaded micelle-embedded polyplexes as a potential treatment of idiopathic pulmonary fibrosis. ACS. Appl. Mater. Interfaces. 17 (8), 11861–11872.
Neary, M.T., et al., 2024. Nebulised delivery of RNA formulations to the lungs: from aerosol to cytosol. J. Control Release 366, 812–833.
Newman, S.P., 2005. Inhaler treatment options in COPD. Eur. Respir. Rev. 14 (96), 102–108.
Omo-Lamai, S., et al., 2024. Physicochemical targeting of lipid nanoparticles to the lungs induces clotting: mechanisms and solutions. Adv. Mater. 36 (26), e2312026.
Schoenmaker, L., et al., 2021. mRNA-lipid nanoparticle COVID-19 vaccines: structure and stability. Int. J. Pharm. 601, 120586.
Szabova, J., et al., 2021. Influence of liposomes composition on their stability during the nebulization process by vibrating mesh nebulizer. Colloids. Surf. B Biointerfaces. 204, 111793.
van Rijn, C.J.M., et al., 2023. Low energy nebulization preserves integrity of SARS-CoV-2 mRNA vaccines for respiratory delivery. Sci. Rep. 13 (1), 8851.
Viger-Gravel, J., et al., 2018. Structure of lipid nanoparticles containing siRNA or mRNA by dynamic nuclear polarization-enhanced NMR spectroscopy. J. Phys. Chem. B 122 (7), 2073–2081.
Wei, T., et al., 2023. Lung SORT LNPs enable precise homology-directed repair mediated CRISPR/Cas genome correction in cystic fibrosis models. Nat. Commun. 14 (1), 7322.
Xu, Y., et al., 2021. Inhaled RNA therapeutics for obstructive airway diseases: recent advances and future prospects. Pharmaceutics 13 (2).
Xue, L., et al., 2024. High-throughput barcoding of nanoparticles identifies cationic, degradable lipid-like materials for mRNA delivery to the lungs in female preclinical models. Nat. Commun. 15 (1), 1884.
Zhang, H., et al., 2020. Aerosolizable lipid nanoparticles for pulmonary delivery of mRNA through design of experiments. Pharmaceutics 12 (11).